Received: 19 December 2019 | Revised: 12 February 2020 | Accepted: 18 February 2020

DOI: 10.1002/cche.10273

NOTE

Zearalenone-malonyl-glucosides as phase II metabolites in plant cell suspension cultures

Beate N. Kohn | **Mirko Bunzel**

Department of Food Chemistry and Phytochemistry, Karlsruhe Institute of Technology (KIT), Institute of Applied Biosciences, Karlsruhe, Germany

Correspondence
Mirko Bunzel, Department of Food Chemistry and Phytochemistry, Karlsruhe Institute of Technology (KIT), Institute of Applied Biosciences, Adenauerring 20a, 76131 Karlsruhe, Germany.
Email: mirko.bunzel@kit.edu

Abstract

Background and objectives: Conjugation of mycotoxins in the phase II metabolism of plants results in modified mycotoxins such as glucosides and malonyl-glucosides. However, malonyl-glucosides have not yet been completely elucidated for zearalenone (ZEN). Thus, the aim of this study was to produce and isolate malonyl-glucosides of ZEN for an unambiguous identification by NMR spectroscopy.

Findings: Zearalenone was incubated in plant cell suspension cultures of wheat, soy, and tobacco, and phase II metabolites were analyzed by using LC-DAD-MS, -HRMS, and NMR spectroscopy. Four main metabolites of ZEN were detected in the cell extracts and identified as two glucosides (attached in positions 14 and 16) and their 6´-malonyl derivatives.

Conclusions: Zearalenone-malonyl-glucosides should be incorporated in future analyses of modified mycotoxins because of their potential relevance for food and feed safety.

Significance and novelty: For the first time, the structures of the two malonyl-glucosides of ZEN were unambiguously identified by NMR spectroscopy after preparative isolation as 14-*O*-(6'-*O*-malonyl-β-D-glucopyranosyl)ZEN and 16-*O*-(6'-*O*-malonyl-β-D-glucopyranosyl)ZEN.

KEYWORDS

malonyl-glucosides, masked mycotoxins, modified mycotoxins, plant cell suspension culture, zearalenone

1 | INTRODUCTION

Besides deoxynivalenol, ZEN is the most common mycotoxin found in cereal crops such as corn, wheat, oats, and barley. ZEN was also detected in peanuts, soy, and other foodstuff (Maragos, 2010). The EFSA Panel on Contaminants in the Food Chain concluded that ZEN causes estrogenic effects, and ZEN can be considered as clastogenic substance (EFSA, 2011; Galloway et al., 1987; Ouanes, Ayed-Boussema, Baati, Creppy, & Bacha, 2005). Consequently, maximum limits for ZEN in cereals and cereal-based products have been established by the European Union (Commission Regulation (EC) No 1881/2006).

However, ZEN can be extensively metabolized in crops, which has been investigated in maize cell suspension cultures in an early study by Engelhardt, Zill, Wohner, and Wallnöfer (1988). Consequently, the reductive phase I metabolites α- and β-ZEL were found in cereal-based food products and feed

(De Boevre et al., 2012). ZEN and its reductive derivatives can further be conjugated by plants or fungi, forming glucosides and sulfates (De Boevre et al., 2012; Nathanail et al., 2015). Some of these metabolites were recently found in Tempeh-like products, which were formed by fungal fermentation of soybeans and maize with ZEN-producing strains (Borzekowski et al., 2019).

Some of the plant-based phase II conjugates such as ZEN-14-glucoside and ZEN-16-glucoside were unambiguously identified by NMR spectroscopic methods in the past (Borzekowski et al., 2018; Kamimura, 1986; Kovalsky Paris et al., 2014), whereas others were only characterized by MS. For example, malonyl-glucosides of ZEN were detected in artificially infested plants by MS methods (Berthiller et al., 2006; Kovalsky Paris et al., 2014). However, unambiguous identification of their structures is essential for producing reference compounds and to conduct bioavailability and toxicological studies.

Bioavailability studies of ZEN-14- and ZEN-16-glucosides have been performed using Caco-2 cells demonstrating a release of the aglycone ZEN and a resorption to the basolateral compartment (Cirlini et al., 2016). Recently, ZEN-14-glucoside and ZEN-16-glucoside were demonstrated to be highly bioavailable and completely hydrolyzed in the gastrointestinal tract of pigs suggesting its contribution to total systemic ZEN toxicity (Binder et al., 2017; Catteuw et al., 2019). As these mechanisms may also apply to malonyl-glucosides, the aim of this study was to analyze the metabolism of ZEN, with a focus on the formation of malonyl-glucosides. Plant cell suspension cultures are suitable tools to obtain larger quantities of metabolites. To consider potentially different metabolic pathways in various plants, cell cultures of wheat, soy, and tobacco (the latter as a well-established plant cell suspension model) were applied to produce and to isolate the main metabolites for unambiguous identification by NMR spectroscopy.

2 | MATERIALS AND METHODS

2.1 | Chemicals and reagents

Zearalenone (purity >98%, by HPLC) was purchased from Fermentek Ltd (Jerusalem, Israel). All other chemicals and reagents were of the highest quality available. Solvents were, if necessary, HPLC-MS grade.

2.2 | Cultivation of plant cell suspension cultures

Wheat cells *(Triticum aestivum* L. emend. Fiori et Paol. cv. Heines Koga II) and soy cells (*Glycine max.* (L.) Merr. cv. Mandarin) were purchased from Leibniz-Institute DSMZ—German Collection of Microorganisms and Cell Cultures. Tobacco BY-2 cells (*Nicotiana tabacum* L. cv. Bright Yellow 2) were kindly provided by the Institute of Botany, KIT. Cells were cultured in 100-ml Erlenmeyer flasks containing 30 ml of modified Gamborg B5 medium (wheat and soy cells) or modified Murashige and Skoog medium (tobacco BY-2 cells) in the dark at 25°C on an orbital shaker at 140 rpm. The Murashige and Skoog medium (pH 5.7) was supplemented with 30 g/L sucrose, 200 mg/L KH_2PO_4, 100 mg/L inositol, 1 mg/L thiamine, and 0.2 mg/L 2,4-dichlorophenoxyacetic acid and the Gamborg-B5 medium (pH 5.5) with 20 g/L sucrose and 2.0 mg/L 2,4-dichlorophenoxyacetic acid. Tobacco BY-2 cells and soy cells were subcultured weekly and wheat suspension cells after 2 weeks.

2.3 | Incubation of plant cell cultures with ZEN

Suspension cells were incubated 4 days after subcultivation in the presence of 150 µl of 10 mM ZEN solution (in DMSO), resulting in DMSO concentrations below 1%. In total, approximately 150 mg of ZEN was used for all incubation experiments described here. Control incubations were performed with DMSO but without ZEN. Seven days after subcultivation, tobacco BY-2 and soy cell suspension cultures were divided into two separate 100-ml Erlenmeyer flasks and 15 ml of fresh medium was added to each flask (wheat cell suspension culture was retained in the original flask without adding fresh medium). Subsequently, another 150 µl of 10 mM ZEN solution was added to the cell suspension cultures. After 6 days of incubation, cells and medium were separated by filtration, cells of the same batch were combined, and cells and media were freeze-dried (overall incubation time was 9 days). Dried media were dissolved in methanol (MeOH) for chromatographic analysis.

2.4 | Extraction procedure of incubated plant cells

Dried cells were ground using mortar and pestle and extracted three times for 1 hr at 25°C to obtain ZEN and its polar metabolites: (a) 4.5 ml MeOH/CH_2Cl_2 (2:1, v/v) per 0.1 g of the ground material; (b) 4.5 ml of MeOH/H_2O/acetic acid (79/20/1, v/v/v); and (c) 4.5 ml of MeOH/CH_2Cl_2 (2:1, v/v). Combined extracts (after centrifugation) were evaporated to dryness, and re-dissolved in 0.2 ml of MeOH to be analyzed by LC-DAD-MS and LC-DAD-HRMS.

2.5 | LC-MS analysis

Gradient elution parameters and more detailed MS parameters are given in the Supporting Information. LC-DAD-MS

analysis was performed on an LXQ Linear Ion Trap MS^n system (Thermo Fisher Scientific) equipped with a Finnigan Surveyor HPLC-DAD system. Separation was carried out on a reversed-phase column (Phenomenex Luna, C18(2), 5 µm, 100 Å, 250 × 4.6 mm i.d.). Metabolites were detected at 239 and 280 nm and characterized with MS (ESI negative or positive mode). Full scan mass spectra were recorded in the range of *m/z* 100 − 1,000, and MS^2 experiments of selected $[M + H]^+$ and $[M - H]^-$ ions were conducted.

LC-DAD-HRMS analyses (same column as above) were performed on a TripleTOF 5,600 Mass spectrometer (AB Sciex) equipped with a 1,290 Infinity LC system (Agilent), software: Analyst TF 1.6.0. The DuoSpray Source was operated in negative ESI mode. MS full scans were recorded from *m/z* 100 to 1,000, and MS/MS spectra (product ions) were recorded from *m/z* 50 to 1,000. Exact and measured accurate masses of the four isolated metabolites are summarized in Table S1.

2.6 | Isolation and purification of glucosides and malonyl-glucosides of ZEN

About 4 g of dry cells was collected from several incubations of each plant cell suspension culture. Freeze-dried and ground cells were extracted by scaling up the procedure described above, yielding about 10 ml of methanolic crude extracts, which were fractionated using preparative RP-HPLC-UVD (LC-8A pumps, SPD-20A UV detector, Shimadzu; Phenomenex, Luna C18(2), 5 µm, 100 Å, 250 × 25.0 mm i.d.): Solvent A: acetonitrile (0.1% formic acid), and solvent B: H_2O (0.1% formic acid), flow rate: 8 ml/min. The linear gradient started with 10% A and was ramped to 30% A in 35 min, ramped to 55% A in 10 min, then ramped to 100% A in 5 min, held for 5 min, decreased to 10% A in 2 min, and followed by an equilibration. ZEN metabolite containing fractions were collected manually, evaporated to about half of their volume, and freeze-dried. The purity of the ZEN metabolites was >97% based on LC-UVD analysis at 280 nm.

2.7 | NMR spectroscopy

NMR spectra (^1H, COSY, HSQC, and HMBC experiments; standard Bruker pulse sequences; 298 K) were recorded on a Bruker Ascend 500 spectrometer equipped with a Prodigy cryoprobe. Freeze-dried samples were usually measured in 500 µl of DMSO-d_6, whereas low-concentrated metabolites were dissolved in 220 µl of DMSO-d_6 and measured in a 5-mm Shigemi NMR tube matched for DMSO-d_6. Low-concentrated samples were analyzed applying non-uniform sampling (NUS), a reduction of 25 to a maximum of 50% was set. Chemical shifts (δ) were referenced to the central solvent signals (δ_H 2.50 ppm and δ_C 39.5 ppm).

3 | RESULTS AND DISCUSSION

3.1 | Metabolite patterns of ZEN obtained from plant cell suspension cultures

Zearalenone (Figure 1) was incubated in wheat (order of Poales), soy (order of Fabales), and tobacco BY-2 (order of Solanales) suspension cells to analyze the metabolism of ZEN in various plant systems, with wheat and soy plants and products being positively analyzed for ZEN in the past. After 9 days of incubation, only trace amounts of ZEN were detected in the incubation media suggesting its extensive uptake into cells. Also, only small amounts of parental ZEN were present in the cell extracts, indicating an active metabolism of ZEN by the cells as also suggested by several additional peaks in the LC chromatograms representing potential ZEN metabolites (Figure 2). Potential ZEN metabolites in the cell extracts were identified by comparing the LC chromatograms with chromatograms obtained from control incubations (incubations without ZEN). Thus, peaks a-d (Figure 2) represent the major metabolites of ZEN. Based on *m/z* values of the quasi-molecular ions and fragmentation patterns in the MS^2 mode, peaks a and c appeared to be ZEN hexosides (*m/z* 479, $[M - H]^-$), whereas peaks b and d suggested ZEN-malonyl-hexosides (*m/z* 565, $[M - H]^-$).

Plant-specific differences are indicated by the metabolite profiles. Whereas tobacco BY-2 cells produce higher amounts of the metabolites represented by the peaks a and d than metabolites represented by the peaks b and c (assuming a comparable response), analysis of the wheat cell extract revealed more comparable amounts of the metabolites represented by the peaks a, c, and d. In contrast to the incubation of tobacco BY-2 and wheat cells, incubation of soy cells with ZEN resulted only in the formation of the metabolites represented by the peaks c and d. Also, tobacco BY-2 cells appeared to produce largest amounts of the metabolites in general (based on peak areas) and may therefore qualify best for the production of relatively high amounts of the two ZEN hexosides and the two ZEN-malonyl-hexosides.

To obtain larger metabolite quantities for unambiguous structural characterization by NMR spectroscopy and HRMS, extracts of several incubations of all three cell cultures were combined and fractionated. Due to low amounts, weighing of the metabolite fraction and of particular metabolites was not feasible. However, rough estimates of the amounts via UV absorption of the sum of the four mentioned metabolites indicated alternative metabolic pathways.

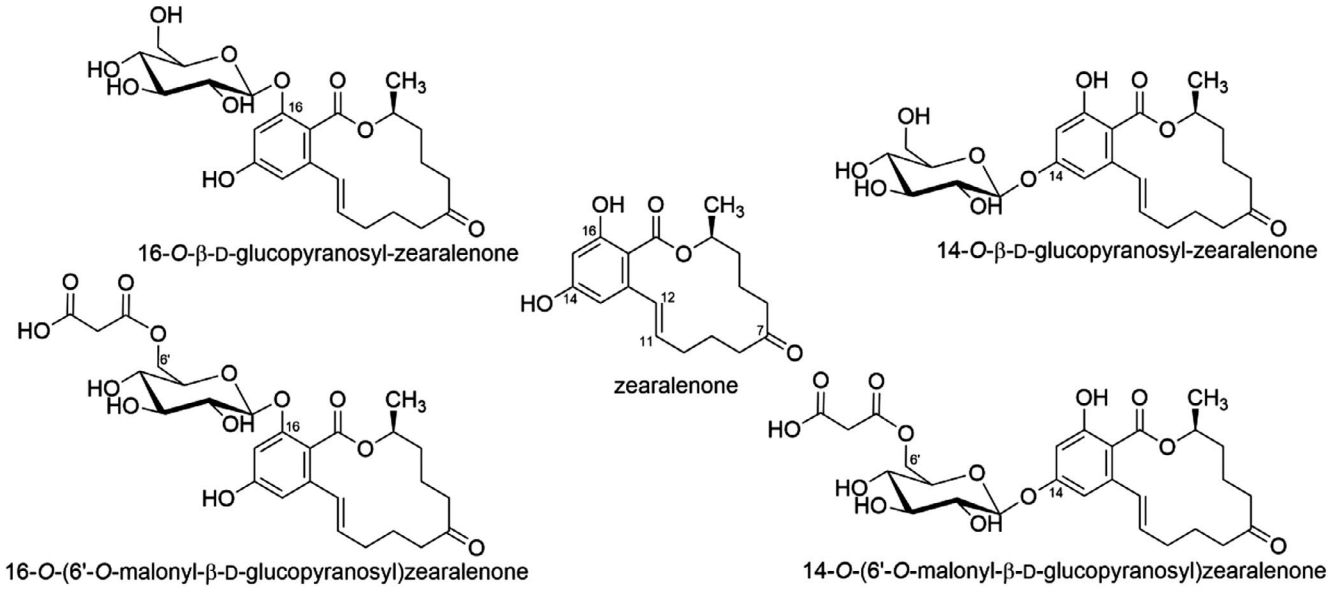

FIGURE 1 Chemical structures of zearalenone (ZEN), 16-*O*-β-D-glucopyranosyl-ZEN, 16-*O*-(6'-*O*-malonyl-β-D-glucopyranosyl)ZEN, 14-*O*-β-D-glucopyranosyl-ZEN, and 14-*O*-(6'-*O*-malonyl-β-D-glucopyranosyl)ZEN

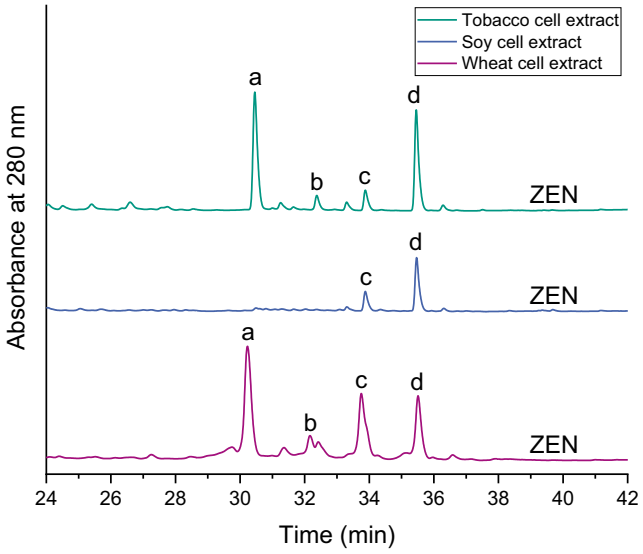

FIGURE 2 HPLC profiles of metabolites of zearalenone (ZEN) in extracts (combined from several extractions) of cultured tobacco BY-2, soy, and wheat cells after 9 days of incubation (UV detection at 280 nm). The marked peaks represent 16-*O*-β-D-glucopyranosyl-ZEN (peak a), 16-*O*-(6´-*O*-malonyl-β-D-glucopyranosyl)ZEN (peak b), 14-*O*-β-D-glucopyranosyl-ZEN (peak c), and 14-*O*-(6´-*O*-malonyl-β-D-glucopyranosyl)ZEN (peak d)

3.2 | Structure elucidation of the main ZEN conjugates

3.2.1 | ZEN-Glucosides

Two ZEN hexosides were unambiguously identified as ZEN-14-glucoside and ZEN-16-glucoside earlier (Borzekowski et al., 2018; Kamimura, 1986; Kovalsky Paris et al., 2014). Here, by using MS and NMR spectroscopy (NMR data: Table 1), the first eluting ZEN-hexoside (peak a) was identified as 16-*O*-β-D-glucopyranosyl-ZEN. Identification of the compound represented by peak c was more challenging due to its low concentration. However, application of a Shigemi tube and NUS enabled full NMR spectroscopic identification. MS and NMR data confirmed the isolated compound c to be 14-*O*-β-D-glucopyranosyl-ZEN.

3.2.2 | ZEN-Malonyl-Glucosides

In the past, ZEN-malonyl-glucosides have only been suggested from MS analysis, missing NMR spectroscopic identification. Here, LC-MS analyses of the metabolites represented by the peaks b and d resulted in the formation of quasi-molecular ions with *m/z* 567 ($[M - H]^-$). The MS^2 spectra showed a loss of 248 Da resulting in fragments with *m/z* 317 $[ZEN - H]^-$, suggesting the elimination of an anhydro-malonyl-glucoside. The elemental composition was calculated on the basis of the measured accurate masses and the isotopic patterns, resulting in $C_{27}H_{34}O_{13}$ being consistent with ZEN-malonyl-hexoside. Interpretation of the ^1H- and 2D-NMR spectra of the two metabolites confirmed the linkage of a malonyl group to the glucose unit: Besides signals in the carbohydrate region of the HSQC spectrum of the metabolite represented by peak b, an additional methylene signal occurred at δ_H 3.25 ppm and δ_C 42.9 ppm, representing the malonic acid CH_2-group. The linkage of a hexose (glucose) to ZEN at position 16 was identified through the HMBC correlation signal between the anomeric proton signal (δ_H

TABLE 1 ^{1}H and ^{13}C NMR shifts of ZEN, 16-*O*-β-D-glucopyranosyl-ZEN, 14-*O*-β-D-glucopyranosyl-ZEN, 16-*O*-(6′-*O*-malonyl-β-D-glucopyranosyl)ZEN, and 14-*O*-(6′-*O*-malonyl-β-D-glucopyranosyl)ZEN

	ZEN			ZEN–16-glucoside			ZEN–14-glucoside			ZEN–6′-malonyl–16-glucoside			ZEN–6′-malonyl–14-glucoside		
	δ_H (ppm)	J (Hz)	δ_C (ppm)	δ_H (ppm)	J (Hz)	δ_C (ppm)	δ_H (ppm)	J (Hz)	δ_C (ppm)	δ_H (ppm)	J (Hz)	δ_C (ppm)	δ_H (ppm)	J (Hz)	δ_C (ppm)
1			169.0			166.8			168.3			167.1			167.8
2	1.27	d (6.2)	19.8	1.25	d (6.3)	19.3	1.27	d (6.1)	19.6	1.25	d (6.4)	19.4	1.26	d (6.2)	19.5
3	4.99	m	71.6	5.13	m	70.5	5.06	m	71.4	5.11	m	70.7	5.08	m	71.0
4	1.49 & 1.60	m	33.9	1.46 & 1.64	m	34.0	1.51 & 1.64	m	34.1	1.46 & 1.63	m	34.1	1.50 & 1.65	m	34,0
5	1.58 & 1.67	m	20.7	1.43 & 1.64	m	20.4	1.51 &1.74	m	20.7	1.44 & 1.68	m	20.5	1.57 & 1.76	m	20.8
6	2.39 & 2.46	m	36.0	2.16 & 2.42	m	43.06	2.28 & 2.30	m	42.8	2.16 & 2.42	m	43.1	2.26 & 2.32	m	42.9
7			211.0			210.4			212.0			211.0			212.0
8	2.18 & 2.38	m	42.6	2.17 & 2.55	m	36.7	2.38 & 2.44	m	36.4	2.17 & 2.56	m	36.8	2.32 & 2.50	m	36.3
9	1.64 & 1.72	m	20.3	1.50 & 1.87	m	20.9	1.64 & 1.71	m	20.7	1.47 & 1.87	m	20.9	1.49 & 1.65	m	20.5
10	2.11	m	30.4	1.89 & 2.26	m	30.6	2.03 & 2.17	m	30.7	1.89 & 2.26	m	30.7	1.99 & 2.21	m	30.6
11	5.79	m	131.7	5.99	ddd (15.7 & 9.8 & 4.2)	132.5	6.00	m	132.8	5.99	ddd (15.7 & 9.7 & 4.3)	132.0	6.01	ddd (15.5 & 9.1 & 6.0)	132.5
12	6.59	d (15.5)	130.5	6.13	d (15.7)	127.6	6.44	d (14.8)	129.3	6.12	d (15.7)	127.8	6.37	d (15.5)	129.1
13	6.37	d (2.2)	105.5	6.58	d (1.8)	104.0	6.68	d (2.1)	104.8	6.53	d (1.6)	104.4	6.61	d (1.6)	104.0
14			160.3			159.0			159.6			160.2			158.9
14-OH	10.03	s		9.84	s					8.13	s				
15	6.22	d (2.2)	101.3	6.48	d (1.8)	100.9	6.45	d (2.1)	102.4	6.59	d (1.6)	101.3	6.49	d (1.6)	102.3
16			169.0			154.7			159.2			155.6			157.3
16-OH	10.86	s					10.61	s					10.61	s	
17			105.6			115.0			111.4			115.0			112.6
18			139.6			135.7			138.3			135.9			137.3
1′				4.81	d (7.5)	99.7	4.89	d (7.6)	99.8	4.75	d (7.0)	100.5	4.90	d (6.9)	99.7

(Continues)

TABLE 1 (Continued)

	ZEN			ZEN–16-glucoside			ZEN–14-glucoside			ZEN–6´-malonyl–16-glucoside			ZEN–6´-malonyl–14-glucoside		
	δ_H (ppm)	J (Hz)	δ_C (ppm)	δ_H (ppm)	J (Hz)	δ_C (ppm)	δ_H (ppm)	J (Hz)	δ_C (ppm)	δ_H (ppm)	J (Hz)	δ_C (ppm)	δ_H (ppm)	J (Hz)	δ_C (ppm)
2´				3.13		73.2	3.20		72.9	3.15		73.4	3.23		72.8
3´				3.23		76.7	3.27		76.3	3.26		76.9	3.29		75.9
4´				3.16		69.2	3.14		69.4	3.11		70.0	3.15		69.5
5´				3.26		76.8	3.33		76.9	3.56		74.0	3.64		73.5
6´				3.67 & 3.48		60.3	3.45 & 3.68		60.4	3.97 & 4.47		63.6	4.06 & 4.39		63.8
Mal-CH_2										3.25		42.9	3.30		41.4
Mal-COOR												167.5			166.7
Mal-COOH										nd		168.8	nd		167.7

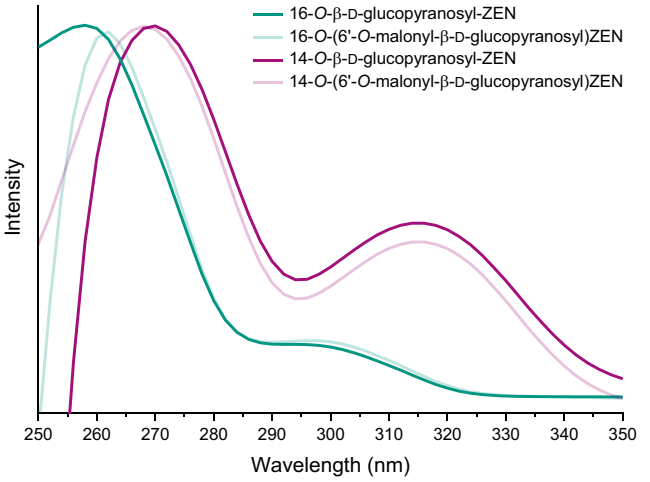

FIGURE 3 Absorption spectra of the four main metabolites of zearalenone (ZEN) in methanol

4.75 ppm) and C16 of ZEN (δ_C 155.6 ppm). NMR data of the ZEN moiety of this metabolite were closely comparable to those of 16-*O*-β-D-glucopyranosyl-ZEN, whereas downfield shifts of H6/C6 and also of H5/C5 in the glucose moiety indicated an electron-withdrawing group in the environment (Figure S1). Correlation peaks in the HMBC spectrum confirmed the malonyl group being attached to the glucose 6 position. The coupling constant of the anomeric proton (7.0 Hz) demonstrated that glucose is in its β-configuration, and the pyranose form was confirmed by the HMBC correlation peak between C5 (δ_C 74.0 ppm) and H1 (4.75 Hz) of the glucose unit. Therefore, the compound represented by peak b was identified as 16-*O*-(6´-*O*-malonyl-β-D-glucopyranosyl)ZEN (Figure 1).

The HSQC spectrum of the second potential ZEN-malonyl-glucoside (represented by peak d) showed a CH_2 signal at δ_H 3.30 ppm and δ_C 41.4 ppm, which, in line with MS data, was assigned to malonic acid. NMR data of metabolite d were closely comparable to those of 14-*O*-β-D-glucopyranosyl-ZEN except for the downfield shifts of H6/C6 and H5/C5 in the glucose moiety. The linkage positions between ZEN, glucose, and the malonyl group were unambiguously identified by HMBC signals. Again, the glucose ring form and its β-configuration were unambiguously assessed by NMR data identifying this compound as 14-*O*-(6´-*O*-malonyl-β-D-glucopyranosyl)ZEN.

Both ZEN-malonyl-glucosides were stable during the measurement period of 2 weeks at −20°C. Köster, Strack, and Barz (1983) as well as Svehliková et al. (2004) reported the instability of several flavonoid-based malonyl-glucosides indicating a possible instability of ZEN-malonyl-glucosides at ambient temperature, which, however, has not been further studied here. Potential breakdown products may be acetyl-glucosides, which were described to occur in micropropagated durum wheat leaf that was artificially contaminated with

ZEN (Righetti et al., 2018). Future studies on the stability of ZEN-malonyl-glucosides and their presence or the presence of ZEN-malonyl-glucoside degradation products in food and feed are therefore recommended.

3.3 | UV-spectra of the identified metabolites

Recording UV absorption spectra of the four main metabolites of ZEN in MeOH revealed that absorption maxima shifted depending on the linkage position of the glucose moiety. With glucose being attached in position C14, the maxima were at about 270 and 314 nm, whereas glucose attachment in position C16 shifted the maxima to about 260 and 300 nm (Figure 3). These differences in the UV absorption spectra become relevant when ZEN and its metabolites are analyzed based on UV detection, implying that specific extinction coefficients are required for every metabolite. A simplified quantitation based on the extinction coefficient of ZEN will inevitably result in inaccurate data. Therefore, no true quantitation of the metabolites based on UV absorption was carried out.

4 | CONCLUSIONS

Zearalenone is efficiently metabolized in wheat, soy, and tobacco BY-2 plant cell cultures with glucosides and malonyl-glucosides being the main metabolites. Malonylation of glucosides in plants is well known and has been observed for flavonoids and pesticides, and, more recently, for two *Alternaria* toxins alternariol and alternariol monomethyl ether in tobacco BY-2 cell suspension cultures (Kogawa, Kazuma, Kato, Noda, & Suzuki, 2007; Taguchi et al., 2010; Hildebrand et al., 2015). Thus, malonylation plays a major role not only for flavonoids and other secondary plant metabolites, but also for xenobiotic compounds such as mycotoxins.

Harms (1992) demonstrated that the metabolism of different pesticides and other xenobiotic compounds in cell suspension cultures was comparable to the metabolism in the corresponding complete plants. Therefore, it can be suggested that ZEN-malonyl-glucosides also occur in naturally contaminated wheat and soy plants. This hypothesis is supported by a study of Rolli et al. (2018) detecting malonyl conjugates of ZEN in leaves and roots of micropropagated Durum wheat by using HRMS analysis. As malonylation was demonstrated to serve as a signal for vacuolar transport (Zhao et al., 2011), it can be hypothesized that malonylated ZEN-glucosides are stored in the vacuole, too. However, in order to better understand the metabolism of ZEN in the plant cell (including phase III reactions/processes) additional kinetic studies are required.

Because it was demonstrated in vitro and in vivo that glucosidic ZEN metabolites are deconjugated during digestion resulting in the aglycone ZEN, the gastrointestinal release of ZEN from malonyl-glucosides appears to be likely (Cirlini et al., 2016; Rolli et al., 2018). Thus, in order to evaluate the potential risk based on ZEN-malonyl-glucosides in food and feed, toxicological studies are required. Also, there is a need to study the natural occurrence of ZEN-malonyl-glucosides in order to confirm the hypothesis of being main metabolites of ZEN in whole plants.

ACKNOWLEDGMENTS

The authors are grateful to Dr. Jan Maisch (Institute of Botany, KIT, Karlsruhe, Germany) for providing BY-2 cells. Also, the authors would like to thank Dr. Sebastian Soukup (Department of Safety and Quality of Fruit and Vegetables, Max Rubner-Institut, Karlsruhe, Germany) for technical assistance with HRMS analyses.

CONFLICT OF INTEREST

The authors declare that they have no conflict of interest.

ORCID

Mirko Bunzel https://orcid.org/0000-0003-0462-8076

REFERENCES

Berthiller, F., Werner, U., Adam, G., Krska, R., Lemmens, M., Sulyok, M., … Schuhmacher, R. (2006). Formation of masked *Fusarium* mycotoxins in plants. *Ernährung*, *30*, 477–481.

Binder, S. B., Schwartz-Zimmermann, H. E., Varga, E., Bichl, G., Michlmayr, H., Adam, G., & Berthiller, F. (2017). Metabolism of zearalenone and its major modified forms in pigs. *Toxins*, *9*, 1–15. https://doi.org/10.3390/toxins9020056

Borzekowski, A., Anggriawan, R., Auliyati, M., Kunte, H.-J., Koch, M., Rohn, S., … Maul, R. (2019). Formation of zearalenone metabolites in Tempeh fermentation. *Molecules*, *24*, 1–14. https://doi.org/10.3390/molecules24152697

Borzekowski, A., Drewitz, T., Keller, J., Pfeifer, D., Kunte, H.-J., Koch, M., … Maul, R. (2018). Biosynthesis and characterization of zearalenone-14-Sulfate, zearalenone-14-glucoside and zearalenone-16-glucoside using common fungal strains. *Toxins*, *10*, 104. https://doi.org/10.3390/toxins10030104

Catteuw, A., Broekaert, N., De Baere, S., Lauwers, M., Gasthuys, E., Huybrechts, B., … Croubels, S. (2019). Insights into *in vivo* absolute oral bioavailability, biotransformation, and toxicokinetics of zearalenone, α-zearalenol, β-zearalenol, zearalenone-14-glucoside, and zearalenone-14-sulfate in pigs. *Journal of Agricultural and Food Chemistry*, *67*, 3448–3458. https://doi.org/10.1021/acs.jafc.8b05838

Cirlini, M., Barilli, A., Galaverna, G., Michlmayr, H., Adam, G., Berthiller, F., & Dall'Asta, C. (2016). Study on the uptake and deglycosylation of the masked forms of zearalenone in human intestinal Caco-2 cells. *Food and Chemical Toxicology*, *98*, 232–239. https://doi.org/10.1016/j.fct.2016.11.003

De Boevre, M., Di Mavungu, J. D., Landschoot, S., Audenaert, K., Eeckhout, M., Maene, P., … De Saeger, S. (2012). Natural

occurrence of mycotoxins and their masked forms in food and feed products. *World Mycotoxin Journal*, *5*, 207–219. https://doi.org/10.3920/WMJ2012.1410

EFSA (2011). Scientific opinion on the risks for public health related to the presence of zearalenone in food. *EFSA Journal*, *9*, 2197.

Engelhardt, G., Zill, G., Wohner, B., & Wallnöfer, P. (1988). Transformation of the *Fusarium* mycotoxin zearalenone in maize cell suspension cultures. *Naturwissenschaften*, *75*, 309–310. https://doi.org/10.1007/BF00367324

Galloway, S. M., Armstrong, M. J., Reuben, C., Colman, S., Brown, B., Cannon, C., … Zeiger, E. (1987). Chromosome aberrations and sister chromatid exchanges in chinese hamster ovary cells: Evaluations of 108 chemicals. *Environmental and Molecular Mutagenesis*, *10*, 1–35. https://doi.org/10.1002/em.2850100502

Harms, H. H. (1992). *In-vitro* systems for studying phytotoxicity and metabolic fate of pesticides and xenobiotics in plants. *Pesticide Science*, *35*, 277–281. https://doi.org/10.1002/ps.2780350313

Hildebrand, A. A., Kohn, B. N., Pfeiffer, E., Wefers, D., Metzler, M., & Bunzel, M. (2015). Conjugation of the mycotoxins alternariol and alternariol monomethyl ether in tobacco suspension cells. *Journal of Agricultural and Food Chemistry*, *63*, 4728–4736. https://doi.org/10.1021/acs.jafc.5b00806

Kamimura, H. (1986). Conversion of zearalenone to zearalenone glycoside by *Rhizopus* sp. *Applied and Environmental Microbiology*, *52*, 515–519. https://doi.org/10.1128/AEM.52.3.515-519.1986

Kogawa, K., Kazuma, K., Kato, N., Noda, N., & Suzuki, M. (2007). Biosynthesis of malonylated flavonoid glycosides on the basis of malonyltransferase activity in the petals of *Clitoria ternatea*. *Journal of Plant Physiology*, *164*, 886–894. https://doi.org/10.1016/j.jplph.2006.05.006

Köster, J., Strack, D., & Barz, W. (1983). High performance liquid chromatographic separation of isoflavones and structural elucidation of isoflavone 7-*O*-glucoside 6"-malonates from *Cicer arietinum*. *Planta Medica*, *48*, 131–135. https://doi.org/10.1055/s-2007-969907

Kovalsky Paris, M. P., Schweiger, W., Hametner, C., Stückler, R., Muehlbauer, G. J., Varga, E., … Adam, G. (2014). Zearalenone-16-*O*-glucoside - A new masked mycotoxin. *Journal of Agricultural and Food Chemistry*, *62*, 1181–1189.

Maragos, C. M. (2010). Zearalenone occurrence and human exposure. *World Mycotoxin Journal*, *3*, 369–383. https://doi.org/10.3920/WMJ2010.1240

Nathanail, A. V., Syvähuoko, J., Malachová, A., Jestoi, M., Varga, E., Michlmayr, H., … Peltonen, K. (2015). Simultaneous determination of major type A and B trichothecenes, zearalenone and certain modified metabolites in Finnish cereal grains with a novel liquid chromatography-tandem mass spectrometric method. *Analytical and Bioanalytical Chemistry*, *407*, 4745–4755. https://doi.org/10.1007/s00216-015-8676-4

Ouanes, Z., Ayed-Boussema, I., Baati, T., Creppy, E. E., & Bacha, H. (2005). Zearalenone induces chromosome aberrations in mouse bone marrow: Preventive effect of 17β-estradiol, progesterone and vitamin E. *Mutation Research - Genetic Toxicology and Environmental Mutagenesis*, *565*, 139–149. https://doi.org/10.1016/j.mrgentox.2004.10.005

Righetti, L., Dellafiora, L., Cavanna, D., Rolli, E., Galaverna, G., Bruni, R., … Dall'Asta, C., (2018). Identification of acetylated derivatives of zearalenone as novel plant metabolites by high-resolution mass spectrometry. *Analytical and Bioanalytical Chemistry*, *410*, 5583–5592. https://doi.org/10.1007/s00216-018-1066-y

Rolli, E., Righetti, L., Galaverna, G., Suman, M., Dall'Asta, C., & Bruni, R. (2018). Zearalenone uptake and biotransformation in micropropagated *Triticum durum* Desf. plants: A xenobolomic approach. *Journal of Agricultural and Food Chemistry*, *66*, 1523–1532.

Svehliková, V., Bennett, R. N., Mellon, F. A., Needs, P. W., Piacente, S., Kroon, P. A., & Bao, Y. (2004). Isolation, identification and stability of acylated derivatives of apigenin 7-*O*-glucoside from chamomile (*Chamomilla recutita* L. RAUSCHERT). *Phytochemistry*, *65*, 2323–2332.

Taguchi, G., Ubukata, T., Nozue, H., Kobayashi, Y., Takahi, M., Yamamoto, H., & Hayashida, N. (2010). Malonylation is a key reaction in the metabolism of xenobiotic phenolic glucosides in *Arabidopsis* and tobacco. *The Plant Journal*, *63*, 1031–1041.

Zhao, J., Huhman, D., Shadle, G., He, X.-Z., Sumner, L. W., Tang, Y., & Dixon, R. A. (2011). MATE2 mediates vacuolar sequestration of flavonoid glycosides and glycoside malonates in *Medicago truncatula*. *The Plant Cell*, *23*, 1536–1555.

SUPPORTING INFORMATION

Additional supporting information may be found online in the Supporting Information section.

How to cite this article: Kohn BN, Bunzel M. Zearalenone-malonyl-glucosides as phase II metabolites in plant cell suspension cultures. *Cereal Chem*. 2020;00:1–8. https://doi.org/10.1002/cche.10273